PHYSICAL REVIEW B VOLUME 48, NUMBER 19 15 NOVEMBER 1993

Quantum-well states of InAs/AlSb resonant-tunneling diodes

Timothy B. Boykin
Department of Electrical and Computer Engineering, The University of Alabama in Huntsville, Huntsville, Alabama 35899

R. E. Carnahan and R. J. Higgins
School of Electrical Engineering and Microelectronics Research Center, Georgia Institute of Technology, Atlanta, Georgia 30332
(Received 14 June 1993; revised manuscript received 2 August 1993)

We study transmission resonances associated with the $n=1$ quantum-well states of InAs/AlSb resonant-tunneling diodes using an empirical tight-binding model. We find that the transmission tends to be fairly sensitive to the wave vector in the plane of the interface, indicating that the usual expression for the tunneling current (which neglects this explicit dependence) is most likely not a good approximation. We show how this behavior is related to the $E(\mathbf{k})$ relation for the InAs conduction band. Finally, we examine the envelope functions associated with the quasibound states, and discuss how their appearance relates to the orbitals of which they are composed.

I. INTRODUCTION

Resonant-tunneling diodes (RTD's) fabricated in the InAs/AlSb materials system are of interest from both experimental and theoretical viewpoints. On the experimental side, these devices have demonstrated high peak-to-valley current ratios (PVR's) and large current densities, properties which result in superior high-frequency devices.[1] A diode composed of an InAs quantum well and electrodes and AlSb barriers has supported oscillations at 712 GHz and demonstrated a power density vastly superior to that of GaAs/AlAs RTD's.[2] Carnahan *et al.*,[3] have recently reported interesting results on tunneling in a magnetic field in these devices. The small InAs electron effective mass, along with the large Γ- and X-tunneling barriers presented by AlSb makes these devices very attractive for high-frequency operation.[1,2]

Because of their large Γ- and X-tunneling barriers these devices are interesting candidates for theoretical study as well. At low temperatures, the Γ and X valleys of AlSb lie about 2.1 and 1.5 eV, respectively, above the InAs conduction-band minimum.[4] In contrast, the Γ and X valleys of AlAs, respectively, lie approximately 1.0 and 0.2 eV above the GaAs conduction-band minimum, the low AlAs X-valley barrier being highly undesirable for device design.[5] In the GaAs/AlAs system, then, even moderately low-lying states in the quantum well of an RTD may be above the AlAs X-valley minimum and hence show significant "leakage" into the barriers, complicating the interpretation of more complete calculations. Determination of how much of this deviation from a simple envelope-function picture is due to this "leakage" as opposed to other effects, such as conduction-band nonparabolicity, for example, can be difficult. The large barriers in the InAs/AlSb system, however, render such "leakage" a minor concern, even for fairly high-lying quantum-well states. Thus, deviations from "ideal" (effective-mass) behavior often can be traced back to the band structure of InAs itself.

It is essential to study these deviations because many calculations of the tunneling current, the quantity most readily compared with experiments, assume some effective-mass behavior. Typically, this involves ignoring the explicit dependence of the transmission coefficient on $\mathbf{k}_\parallel$ (wave vector in the plane of the interface) in order to make the computation more tractable.[6] Tunneling in single AlAs barriers by electrons with nonzero $\mathbf{k}_\parallel$ is examined by Boykin and Harris[7] and more recently Kiledjian *et al.*,[8] have demonstrated the importance of including $|\mathbf{k}_\parallel|$ in tunneling current calculations for interband tunneling diodes. It is of interest to examine this effect for electron tunneling double-barrier structures as well. For simplicity, we will restrict our study to $\mathbf{k}_\parallel$ lying in the $\mathbf{x}$ direction.[9] We examine both the transmission as a function of bias for electrons of different energies and the flat-band quantum-well states from which the transmission peaks arise. In Sec. II we briefly review our method and set out the assumptions made in the calculations. Section III presents our results and Sec. IV our conclusions.

II. METHOD AND ASSUMPTIONS

We employ the 10-band nearest-neighbor tight-binding model of Vogl, Hjalmarson, and Dow[10] in our study of InAs/AlSb RTD's. We consider devices grown on [001]-oriented substrates and write the wave function as a linear combination of Bloch sums centered on layers, L

$$|\psi_{\mathbf{k}_\parallel}\rangle = \sum_{L,n,t} C_L^{nt} |nt;L;\mathbf{k}_\parallel\rangle \tag{1}$$

where L indexes layers, n indexes orbitals (s,p_x,p_y,p_z,s^*), and t indexes atom type (a for anion or c for cation). The Bloch sums are themselves linear combinations of atomiclike orbitals

$$|nt;L;\mathbf{k}_\parallel\rangle = \frac{1}{\sqrt{N_\parallel}} \sum_{j=1}^{N_\parallel} \exp\{i\mathbf{k}_\parallel\cdot[\mathbf{R}_{j\parallel}(L)+\delta_{t,c}\mathbf{v}_\parallel]\} \times |nt;L;\mathbf{R}_{j\parallel}(L)+\delta_{t,c}\mathbf{v}_\parallel\rangle \ . \tag{2}$$

0163-1829/93/48(19)/14232(6)/$06.00 ©1993 The American Physical Society

The transfer matrix,[11] which relates the coefficients in layer L to those in layer $(L-1)$ is generated by taking matrix elements of the tight-binding Hamiltonian with states (1) and (2). Due to the presence of evanescent transfer-matrix eigenstates it is necessary to use some type of numerical stabilization scheme in calculating the coefficients C_L^{nt} for all but the shortest of structures. The details of our method may be found elsewhere;[6] other methods[12] are also possible. From the coefficients C_L^{nt} we find the transmission and reflection coefficients for tunneling.

Space-charge regions are included in our calculations of transmission versus bias. The charge term in the Poisson equation arises from the donors (which are assumed to be fully ionized) and the electrons, which obey Fermi-Dirac statistics; the density of states used in the Poisson equation assumes a parabolic conduction band. The resulting potential profile is used in the tight-binding solution of the Schrödinger equation; the Schrödinger and Poisson equations are not solved self-consistently. (The Poisson solution is incorporated into the Schrödinger equation as a stepwise-constant potential.) Last, when we study devices under "flatband" conditions we assume zero charge and zero electric field.

There are two further important considerations for InAs/AlSb devices which do not arise for GaAs/AlAs RTD's. The first is lattice matching. While InAs and AlSb are not grossly mismatched, neither are their lattice constants nearly identical as is the case with GaAs and AlAs. We assume that the AlSb in-plane lattice constant is that of bulk InAs and because we are primarily concerned with quantum-well (InAs) states, we ignore strain. The second issue is the nature of the interface; because there are no common atoms between the two constituent materials, InAs and AlSb, the interface can be either InSb- or AlAs-type. We assume that there is associated with each barrier one of each type of interface. The resulting structure then in general has less symmetry than a similar GaAs/AlAs RTD. For example, under flatband conditions a GaAs/AlAs RTD with identical barriers is invariant under rotation by $\pm\pi/2$ about the $\mathbf{z}$ axis followed by a z reflection about the center of the device, where $\mathbf{z}$ denotes the growth direction. In contrast, under our assumptions in similar InAs/AlSb devices one of the barrier-quantum well interfaces is AlAs-type while the other is InSb-type, destroying this symmetry. Nevertheless, as we shall see in the next section, the wave functions of the quantum-well states often display approximate symmetry.

III. RESULTS

Our first topic is the variation of the transmission with $\mathbf{k}_\parallel = \mathbf{k}_x\hat{\mathbf{x}} + k_y\hat{\mathbf{y}}$. As stated in the introduction, one typically replaces the exact current density expression,

$$J_z(V) = \frac{2e}{(2\pi)^3\hbar}\int [f_e(E) - f_c(E)]T(E,\mathbf{k}_\parallel,V)d\mathbf{k}_\parallel dE \ , \tag{3}$$

where V is the applied bias, f_e and f_c are the bulk emitter and collector Fermi-Dirac functions, respectively, and T is the transmission coefficient, the integration being over the incident electron, with the familiar form[13]

$$J_z(V) = \frac{em^* k_B T}{2\pi^2\hbar^3}\int T(E,0,V) \times \ln\left\{\frac{1+\exp[(\mu_e - E)/k_B T]}{1+\exp[(\mu_e - E - eV)/k_B T]}\right\} \times dE \ . \tag{4}$$

In going from (3) to (4), it was necessary to make the replacement

$$T(E,\mathbf{k}_\parallel,V) \rightarrow T(E - E_c(\mathbf{k}_\parallel,0),0,V) \ . \tag{5}$$

We examine the validity of the replacement, (5), by calculating the transmission versus bias for electrons with the same values of $E_z \equiv E - E_c(\mathbf{k}_\parallel,0)$ but differing $\mathbf{k}_\parallel$.

The device under consideration consists of InAs bulk regions, with both emitter collector N doped to 10^{18} cm^{-3}; there is also an undoped emitter spacer and an undoped collector space, each 33 monolayers thick. The InAs well is 15 monolayers wide and each of the two AlSb barriers is 13 monolayers wide; neither the barriers nor the well is doped. The temperature is taken to be 77 K, and the emitter and collector Fermi levels lie about 159 meV above their respective conduction-band minima.

Figures 1–3 present the transmission versus applied bias for electrons of various $\mathbf{k}_\parallel$ with E_z approximately equal to 14, 50, and 157 meV, respectively. Due to the Fermi-Dirac functions in (3) it is only necessary to consider fairly small values of $|\mathbf{k}_\parallel|$. For example, the electron with $\mathbf{k}_\parallel = 0.05\hat{\mathbf{x}}$ Å^{-1} in Fig. 1 lies about 231 meV above the InAs emitter conduction-band minimum; even the electron with $\mathbf{k}_\parallel = 0.01\hat{\mathbf{x}}$ Å^{-1} in Fig. 3 is about 171 meV above the InAs conduction-band minimum. Before examining the validity of (5), let us first comment on some general features of the transmission graphs of Figs. 1–3. Note that all of the resonances are Fabry-Perot–like, indicating that a single-state mechanism is at work; there are none of the notches[14] or Fano-type resonances[15,16] associated with multiple-state wave propagation. As each graph has but one Fabry-Perot–like reso-

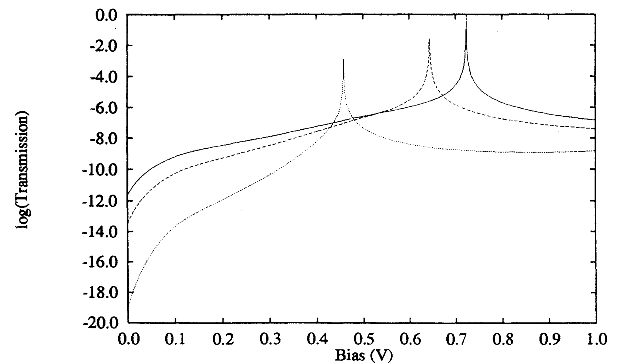

FIG. 1. Base-10 logarithm of the transmission vs applied bias for electrons with $E_z \approx 14$ meV (see text). Solid line: $\mathbf{k}_\parallel = 0$; dashed line: $\mathbf{k}_\parallel = (0.02,0)$ Å^{-1}; dotted line: $\mathbf{k}_\parallel = (0.05,0)$ Å^{-1}.

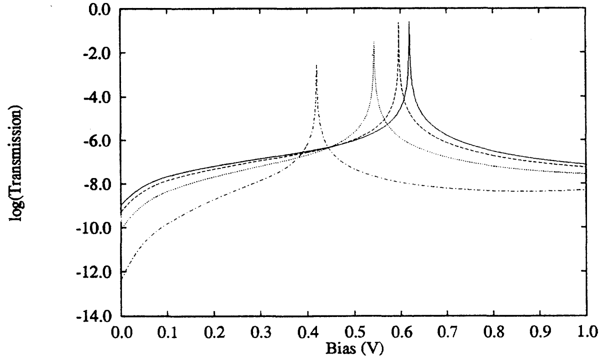

FIG. 2. Base-10 logarithm of the transmission vs applied bias for electrons with $E_z \approx 50$ meV (see text). Solid line: $\mathbf{k}_{\parallel}=0$; dashed line: $\mathbf{k}_{\parallel}=(0.01,0)$ Å^{-1}; dotted line: $\mathbf{k}_{\parallel}=(0.02,0)$ Å^{-1}; dotted-dashed line: $\mathbf{k}_{\parallel}=(0.04,0)$ Å^{-1}.

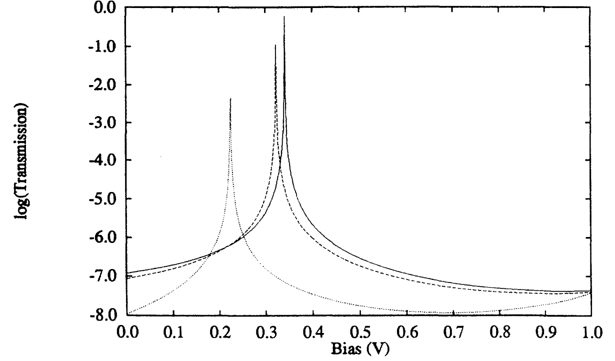

FIG. 3. Base-10 logarithm of the transmission vs applied bias for electrons with $E_z \approx 157$ meV (see text). Solid line: $\mathbf{k}_{\parallel}=0$; dashed line: $\mathbf{k}_{\parallel}=(0.01,0)$ Å^{-1}; dotted line: $\mathbf{k}_{\parallel}=(0.03,0)$ Å^{-1}.

nance, we expect that these peaks are associated with the respective $n=1$ InAs quantum-well states. Later we will show that this is indeed the case.

Table I lists, by figure, the values of $\mathbf{k}_{\parallel}$; E (energy relative to the InAs Γ-valley minimum); $E_z = E - E_c(\mathbf{k}_{\parallel},0)$; approximate peak bias, V_p; and difference between the incident electron energy and that of the middle of the quantum well, ΔE. For the replacement (5) to be valid, all transmission graphs in each figure should nearly coincide since the values of E_z for each figure are almost identical. Evidently, then, the replacement (5) appears rather poor for low-, medium-, and high-E_z electrons. Although we have studied transmission only for $\mathbf{k}_{\parallel}$ of the form $(k_x,0)$, the large magnitude of the discrepancy between actual behavior and that necessary for (5) to be well justified suggests that (4) is probably not a good approximation to (3). Since the graph of current density versus bias may be envisioned as a weighted sum of transmission graphs like those in Figs. 1–3, it appears that (4) likely overestimates the peak current density.[17] We note that Kiledjian *et al.*[8] have drawn similar conclusions for interband tunneling devices.

Having noted the significant departure from ideal behavior exhibited in Figs. 1–3, we now analyze the factors behind it. The task is most easily accomplished by examining the flatband quantum-well states from which the transmission peaks under bias arise. Table II lists the energies of the transmission resonances for a double-barrier RTD with 13-monolayer AlSb barriers, a 15-monolayer InAs well, and InAs bulk regions for various $\mathbf{k}_{\parallel}$ relative to the InAs conduction-band minimum along with $E_z = E - E_c(\mathbf{k}_{\parallel},0)$ and the z wave vector of the Bloch state resonating in the well. (At these energies there are but two Bloch waves, one each at $\pm k_z$.) The electron is incident from the Γ valley of the InAs emitter. As expected, there is close agreement between the values of ΔE in Table I and the values of E in Table II. Note that even under flatband conditions the lowest resonances for different $\mathbf{k}_{\parallel}$ occur at very different values of E_z. On the other hand, the z wave vectors of the Bloch states resonating in the well are all similar. This should not be surprising: resonance is a wave phenomenon. Therefore, we ought to consider k_z to be the more fundamental quantity. The differences in E_z under flatband conditions should hence arise from the InAs $E(\mathbf{k})$ relationship; this is illustrated in Fig. 4, a plot of the InAs conduction band for the values of $\mathbf{k}_{\parallel}$ in Table II versus k_z. Finding the intersection of the line $k_z = 0.055$ Å^{-1} (approximate resonance condition for all $\mathbf{k}_{\parallel}$ considered here) with each of the curves $E(\mathbf{k})$ clearly shows the large differences between the E_z at the various resonances. Thus, the shifts in the transmission graphs for different $\mathbf{k}_{\parallel}$ are seen to be

TABLE I. Quantum-well resonances under bias. See text for explanation of symbols.

Figure	$\mathbf{k}_{\parallel}=(k_x,0)$ (Å^{-1})	E_z (meV)	E (meV)	ΔE (meV)	V_p (V)
1	0.00	13.8	13.8	241.3	0.723
1	0.02	13.7	63.8	264.2	0.643
1	0.05	13.8	231.3	368.4	0.458
2	0.00	50.1	50.1	242.2	0.619
2	0.01	50.3	64.1	248.1	0.596
2	0.02	50.2	100.3	265.3	0.543
2	0.04	50.1	207.0	326.1	0.420
3	0.00	156.9	156.9	244.4	0.341
3	0.01	156.8	170.6	250.2	0.322
3	0.03	156.9	256.8	293.8	0.225

TABLE II. Flatband quantum-well states. See text for explanation of symbols.

$\mathbf{k}_{\parallel}=(k_x,0)$ (Å $^{-1}$)	E_z (meV)	E (meV)	k_z (Å $^{-1}$)
0.00	243.5	243.5	0.05419
0.01	235.5	249.2	0.05431
0.02	215.8	265.9	0.05465
0.03	192.0	291.9	0.05517
0.04	168.7	325.6	0.05581
0.05	147.4	365.0	0.05651

due to the dispersion relation of the InAs conduction band. Last, note that the application of bias will magnify these shifts.

In light of the foregoing discussion, the difficulties with the replacement (5) become clear: the replacement breaks down whenever there is non-negligible in-plane dispersion and the bands are nonparabolic. Note that it is sufficient for the effective mass to depend on E alone—an isotropic, but nonparabolic, conduction band will render (5) invalid. The error in (5) is most easily stated in effective-mass language: it assumes that E and $k_{\parallel}^2/m^*$ are good quantum numbers whereas E and $\mathbf{k}_{\parallel}$ are the actual conserved quantities. The electron effective mass in a device under bias having an isotropic conduction band is then a function of $(E-E_c^{\min}[z])$, where $E_c^{\min}[z]$ is the energy of the conduction-band minimum at the point z. (In a tight-binding description one substitutes the discrete layer index, L, for z.) Since under normal operating conditions the well of a RTD typically lies at least a few tens of millivolts below the bulk emitter conduction-band minimum, two electrons having different E and $|\mathbf{k}_{\parallel}|$ but similar k_z *in the emitter* will usually have very different k_z *in the well* due to the nonparabolicity. It is thus no surprise that their transmission peaks will tend to occur at rather different biases.

It may be helpful to comment briefly on the foregoing results in the context of a two-band tight-binding model[18,19] (one having only s-cation and p_z-anion orbitals).

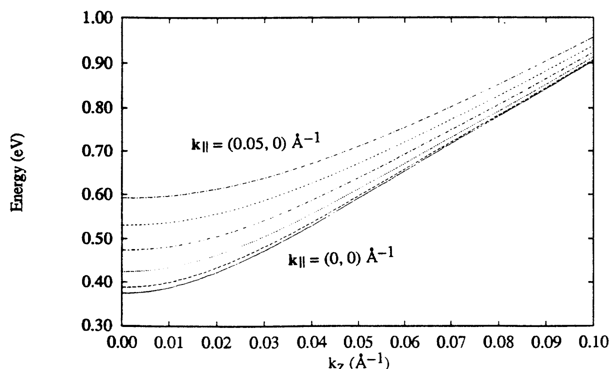

FIG. 4. Conduction-band energies of InAs vs k_z for various $\mathbf{k}_{\parallel}$. Solid line: $\mathbf{k}_{\parallel}=\mathbf{0}$; long dashed line: $\mathbf{k}_{\parallel}=(0.01,0)$ Å $^{-1}$; dotted line: $\mathbf{k}_{\parallel}=(0.02,0)$ Å $^{-1}$; long dotted-dashed line: $\mathbf{k}_{\parallel}=(0.03,0)$ Å $^{-1}$; short dashed line: $\mathbf{k}_{\parallel}=(0.04,0)$ Å $^{-1}$; short dotted-dashed line: $\mathbf{k}_{\parallel}=(0.05,0)$ Å $^{-1}$.

While the two-band model can, for example, closely reproduce the above $\mathbf{k}_{\parallel}=\mathbf{0}$ flatband results,[20] calculations for $\mathbf{k}_{\parallel}\neq\mathbf{0}$ tend to differ significantly from those of the ten-band model, as expected from the lack of p_x and p_y orbitals in the former. Indeed, for the ranges of k_x and k_z considered in this work, the conduction band varies so little with k_x that in a plot like Fig. 4 all six curves lie nearly atop one another. Not surprisingly, in the two-band model the flatband resonances for the six values of $\mathbf{k}_{\parallel}$ listed in Table II all occur at nearly identical values of E. Therefore, the preceding discussion of nonparabolicity and the conservation of $\mathbf{k}_{\parallel}$ versus $k_{\parallel}^2/m^*$, which assumes non-negligible in-plane dispersion, does not apply in the two-band case.

We may confirm that the flatband resonances just discussed are indeed the $n=1$ states by plotting a layer-wise sampling of the probability density in the well for each state. From (1) and (2), then, the density in each type of plane (anion or cation) is just

$$\rho_L^t=\sum_n |C_L^{nt}|^2 , \tag{6}$$

where the sum is again over orbital types and t is either a or c. Thus, the sets $\{C_L^{nt}\}$ represent a layerwise sampling of the various orbital envelope functions while the densities (6) are roughly the square magnitudes of the total anion and cation envelopes. In Figs. 5–7 we present the graphs of the anion and cation densities for the cases $\mathbf{k}_{\parallel}=(0,0)$, (0.03,0), and (0.05,0) Å $^{-1}$, respectively, under flatband conditions. The peak density in the well tends to be higher for larger $|\mathbf{k}_{\parallel}|$ in this regime, but the main barrier state (AlSb Γ valley, evanescent) decays more rapidly for states of larger $|\mathbf{k}_{\parallel}|$ also. In these figures, the first barrier extends from monolayer 22–34; the quantum well from monolayer 35–49; and the second barrier from monolayer 50–62. We note that the envelopes decay rapidly within the barriers, showing no significant oscillation or other signs of a barrier state at these energies. Thus, these are truly quantum well states, as we surmised earlier from the Fabry-Perot–like transmission resonances.

The shapes of the envelopes merit some discussion. Those for the $\mathbf{k}_{\parallel}=(0.05,0)$ Å $^{-1}$ state look much as we might expect an $n=1$ level to appear, given the nonsymmetric interfaces—approximately even about the center of the well. For the $\mathbf{k}_{\parallel}=\mathbf{0}$ state (Fig. 5), however, the anion envelope has two peaks and for the $\mathbf{k}_{\parallel}=(0.03,0)$ Å $^{-1}$ state (Fig. 6) it is nearly flat. [For $\mathbf{k}_{\parallel}=(0.028,0)$ Å $^{-1}$—not shown—it is very flat indeed.] Because in each case the quantum-well state is essentially composed of but one pair of Bloch waves and due to the $\mathbf{k}_{\parallel}$ considered here the interpretation is not too difficult. Recall that since zinc blende is invariant under a twofold rotation about the **x** axis, this operation will relate the forward- and reverse-propagating states with $\mathbf{k}_{\parallel}=(k_x,0)$. In particular, this rotation changes the signs of the p_y and p_z coefficients relative to the others. Therefore, if we construct a linear combination of these two states in which the s envelopes are even about some point z_0 we will find that the s^* and p_x envelopes of the combination are likewise even about this same point but that the p_y

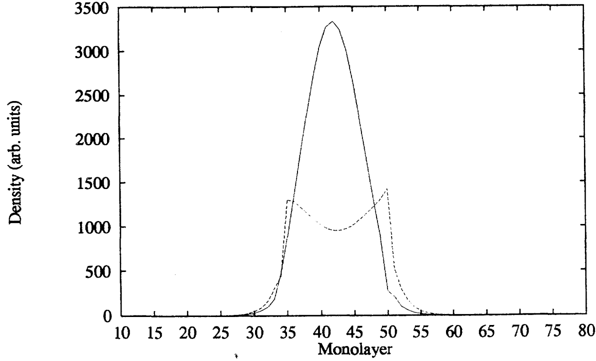

FIG. 5. $n=1$ flatband quantum-well state for the 15-monolayer well device, $\mathbf{k}_{\parallel}=\mathbf{0}$. Solid line: cation density; dashed line: anion density.

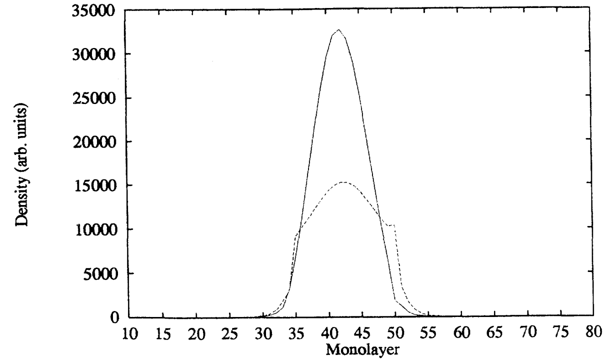

FIG. 7. $n=1$ flatband quantum-well state for the 15-monolayer well device, $\mathbf{k}_{\parallel}=(0.05,0)$ Å $^{-1}$. Solid line: cation density; dashed line: anion density.

and p_z envelopes are odd about it.

In the present case, the Bloch waves in the well are primarily composed of s-, p_z-, and, for the $\mathbf{k}_{\parallel}=(0.03,0)$ and $(0.05,0)$ Å $^{-1}$ states, p_x-like orbitals. Since the barriers are of equal thickness, we expect that the total wave function for the $n=1$ (flatband) state ought to be approximately even about the center of the well. Thus, we should find that the s- and p_x-like envelopes are roughly proportional to $\cos[k_z(z-z_0)]$ where z_0 is the coordinate of the center of the well, while the p_z-like envelope should be approximately proportional to $\sin[k_z(z-z_0)]$. (The envelopes do, in fact, manifest this type of behavior.) The s and p_x densities should thus have one peak each but the p_z density should have two. Since by (6) the anion and cation densities are sums over orbital types, their appearance will indicate the dominant orbital(s) of the Bloch waves in the well. In all three cases (within our parametrization), the major cation contribution to the Bloch states is s-like, hence the cation envelopes have only one peak. For $\mathbf{k}_{\parallel}=\mathbf{0}$, the anion contribution is mainly p_z-like, so there are two peaks, while for $\mathbf{k}_{\parallel}=(0.05,0)$ Å $^{-1}$ the sum of the square magnitudes of the anion s and p_x coefficients of the Bloch waves is larger than the square magnitude of the anion p_z coefficient, leading to a single peak. On the other hand, in the $\mathbf{k}_{\parallel}=(0.03,0)$ Å $^{-1}$ state the sum of the square magnitudes of the anion s and p_x coefficients of the Bloch waves is about the same as the square magnitude of the anion p_z coefficient, so that the anion density is approximately proportional to $\{\sin^2[k_z(z-z_0)]+\cos^2[k_z(z-z_0)]\}=1$, i.e., flat.

We briefly note that because the ten-band model has orbitals not included in the two-band calculation (the s and p_x anion being most relevant to the present discussion), wave function results for the latter will not always resemble those of the former. Considering the $n=1$ states discussed above as definite examples, we anticipate the two-band cation envelopes to resemble those of the ten-band model, whose cation component is s-like. In contrast, we should find that the purely p_z-like two-band anion envelopes for all six $\mathbf{k}_{\parallel}$ states will have two peaks and much lower densities near the well center as compared to the ten-band results. Explicit calculation confirms our intuition.

Structures with wider wells manifest similar behavior, as illustrated in Figs. 8 and 9, which are, respectively, density plots for the $n=1$ and 2 (flatband) states of a device having 13-monolayer AlSb barriers and a 30-monolayer InAs well. (Here, the first barrier extends from monolayer 22–34, the well from 35–64, and the

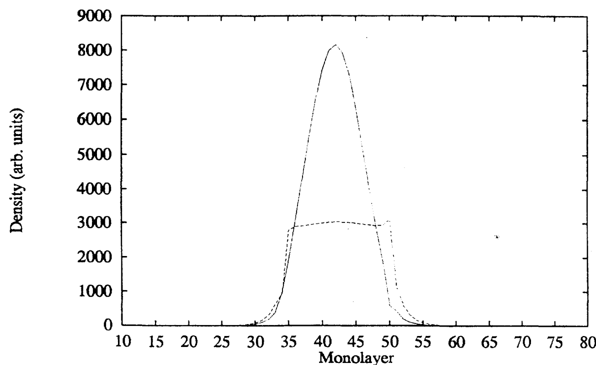

FIG. 6. $n=1$ flatband quantum-well state for the 15-monolayer well device, $\mathbf{k}_{\parallel}=(0.03,0)$ Å $^{-1}$. Solid line: cation density; dashed line: anion density.

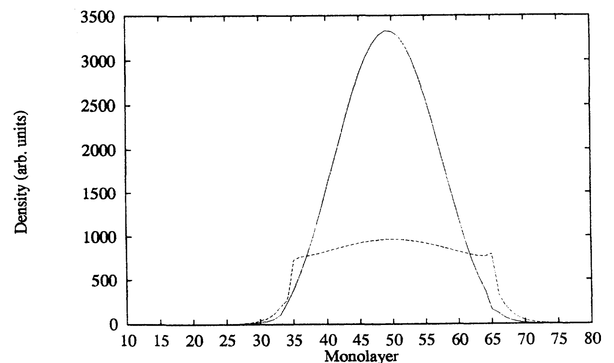

FIG. 8. $n=1$ flatband quantum-well state for the 30-monolayer well device, $\mathbf{k}_{\parallel}=0$. Solid line: cation density; dashed line: anion density.

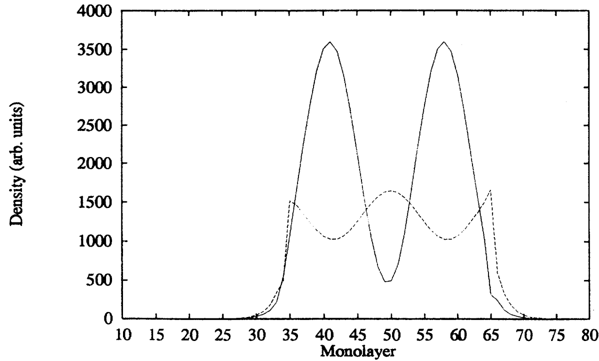

FIG. 9. $n=2$ flatband quantum-well state for the 30-monolayer well device, $\mathbf{k}_{\parallel}=0$. Solid line: cation density; dashed line: anion density.

second barrier from 65–77.) In the lower-energy state (Fig. 8), the Bloch waves in the quantum well are mainly composed of s-like orbitals for both anions and cations. In contrast, in our parametrization the $n=2$ state (Fig. 9) is principally composed of s-like cation orbitals and p_z-like anion orbitals, so the two densities show different numbers of peaks.

IV. CONCLUSIONS

We have examined tunneling in InAs/AlSb double-barrier RTD's for various $\mathbf{k}_{\parallel}$. Our results indicate that the simple single-integral approximation for the tunneling current density, Eq. (4), is likely not very good. In particular, we have presented evidence indicating that it likely overestimates the true peak current density. Evaluation of the full expression (3), is thus expected to predict a more realistic peak current and, hence, PVR. We have analyzed the reasons for the failure of the replacement, Eq. (5), and the deviations from ideal (effective-mass) behavior, tracing them back to the $E(\mathbf{k})$ relation for the InAs conduction band. Finally, we have plotted the probability densities for the flatband states corresponding to the first resonances in the transmission versus bias curves and have seen how their shapes are related to the atomiclike orbitals of which they are composed.

ACKNOWLEDGMENTS

We thank K. P. Martin for useful discussions. T.B.B. gratefully acknowledges the technical assistance rendered by Dr. Rhonda Gaede and Helen Foster of UAH. R.E.C. and R.J.H. acknowledge the support of the NSF through Grant No. ECS-8922512.

[1] L. F. Luo, R. Beresford, and W. I. Wang, Appl. Phys. Lett. **53**, 2320 (1988); D. H. Chow, J. R. Söderström, D. A. Collins, D. Z.-Y. Ting, E. T. Yu, and T. C. McGill, Proc. SPIE **1283**, 2 (1990); J. R. Söderström, E. R. Brown, C. D. Parker, L. J. Mahoney, J. Y. Yao, T. G. Andersson, and T. C. McGill, Appl. Phys. Lett. **58**, 275 (1991).

[2] E. R. Brown, J. R. Söderström, C. D. Parker, L. J. Mahoney, K. M. Molvar, and T. C. McGill, Appl. Phys. Lett. **58**, 2292 (1991).

[3] R. E. Carnahan, M. A. Maldonado, K. P. Martin, A. Nogaret, R. J. Higgins, L. A. Cury, D. K. Maude, J. C. Portal, J. F. Chen, and A. Y. Cho, Appl. Phys. Lett. **62**, 1385 (1993).

[4] Material parameters are from *Semiconductors,* Landolt-Börnstein, New Series, Group III, Vol. 17a, edited by O. Madelung (Springer-Verlag, Berlin, 1982), except for the InAs Γ-valley effective mass, which is from S. M. Sze, *Physics of Semiconductor Devices* (Wiley, New York, 1981), p. 849.

[5] E. E. Mendez, E. Calleja, and W. I. Wang, Appl. Phys. Lett. **53**, 977 (1988).

[6] Timothy B. Boykin, Jan P. A. van der Wagt, and James S. Harris, Jr., Phys. Rev. B **43**, 4777 (1991).

[7] Timothy B. Boykin and James S. Harris, Jr., J. Appl. Phys. **72**, 988 (1992).

[8] M. S. Kiledjian, J. N. Schulman, K. L. Wang, and K. V. Rousseau, Phys. Rev. B **46**, 16 012 (1992).

[9] While our preliminary calculations indicate that for small wave vectors the transmission tends to be fairly insensitive to the direction of $\mathbf{k}_{\parallel}$, a more detailed study, beyond the scope of the present work, is required before drawing firm conclusions in this matter.

[10] P. Vogl, Harold P. Hjalmarson, and John D. Dow, J. Phys. Chem. Solids **44**, 365 (1983).

[11] D. H. Lee and J. D. Joannopoulos, Phys. Rev. B **23**, 4988 (1981); J. Vac. Sci. Technol. **19**, 355 (1981).

[12] D. Z.-Y. Ting, E. T. Yu, and T. C. McGill, Appl. Phys. Lett. **58**, 292 (1991); J. N. Schulman and D. Z.-Y. Ting, Phys. Rev. B **45**, 6282 (1992).

[13] R. Tsu and L. Esaki, Appl. Phys. Lett. **22**, 562 (1973).

[14] Timothy B. Boykin, Bardia Pezeshki, and James S. Harris, Jr., Phys. Rev. B **46**, 12 769 (1992).

[15] U. Fano, Phys. Rev. **124**, 1866 (1961).

[16] Timothy B. Boykin, Phys. Rev. B **47**, 12 696 (1993).

[17] In order to examine the replacement (5) under conditions most favorable to it and to facilitate comparison with the flat-band quantum-well states we calculate $E_c(\mathbf{k}_{\parallel},0)$ using the tight-binding model. In going from (3) to (4) one, in fact, takes $[E_c(\mathbf{k}_{\parallel},0)-E_c(0)]=\hbar^2k_{\parallel}^2/2m^*$ where m^* is the effective mass of the electron in the emitter. As expected, when nonparabolicity in the emitter is important and $\hbar^2k_{\parallel}^2/2m^*$ is significant as compared to E_z, the replacement (5), tends to become *even less* accurate than indicated herein since for a nonparabolic conduction band one typically has $[E_c(\mathbf{k}_{\parallel},0)-E_c(\mathbf{0})]<\hbar^2k_{\parallel}^2/2m^*$. Specifically, for the cases we consider which satisfy the foregoing criteria, taking $[E_c(\mathbf{k}_{\parallel},0)-E_c(\mathbf{0})]=\hbar^2k_{\parallel}^2/2m^*$ results in shifts of the $\mathbf{k}_{\parallel}\neq 0$ curves relative to their respective $\mathbf{k}_{\parallel}=\mathbf{0}$ curves that are even *larger* than those shown in Figs. 1–3.

[18] G. A. Sai-Halasz, L. Esaki, and W. A. Harrison, Phys. Rev. B **18**, 2812 (1978).

[19] J. N. Schulman, J. Appl. Phys. **60**, 3954 (1986).

[20] Close agreement may be obtained by using the $V(pa,sc)$ (notation is that of Ref. 10) interface parameters (one for each type interface) from the ten-band model rather than those appropriate to a two-band model because these latter parameters lead to an unrealistically asymmetric structure. For all other layers, parameters appropriate to the two-band model (i.e., which properly fit both the gap and electron effective mass at Γ of the material in question) should be employed.